# Physical Gelation in a Triblock Copolymer Solution: In Situ Study of Stress−Strain Behavior and Structural Development

**R. Kleppinger,[†,‡] M. van Es,[§] N. Mischenko,[†] M. H. J. Koch,[∥] and H. Reynaers*[,†]**

*Laboratory of Macromolecular Structural Chemistry, Catholic University of Leuven, Celestijnenlaan 200F, B3001 Heverlee, Belgium, DSM Research, Postbus 18, 6160 MD Geleen, The Netherlands, and European Molecular Biology Laboratory, Hamburg Outstation, EMBL c/o DESY, Notkestrasse 85, D-22603 Hamburg, Germany*

*Received January 28, 1998; Revised Manuscript Received May 18, 1998*

ABSTRACT: An in situ study of the microstructure and mechanical properties of polystyrene−poly(ethylene−butylene)−poly styrene (SEBS) triblock copolymer gels was performed. Simultaneous time-resolved synchrotron radiation X-ray scattering and stress−strain measurements at extensions up to $\lambda = 2$ indicate that the macroscopic deformations are transferred to a microscopic level via the three-dimensional network of microdomains. The deformation of the microstructure is nonaffine at low extension rates ($4 \times 10^{-4}$ s$^{-1}$) and becomes affine at higher rates ($10^{-2}$ s$^{-1}$).

## 1. Introduction

It is well documented that di- and triblock copolymers can form micelles in solution, and a number of studies have focused on micellization of AB- and ABA-type block copolymers in solvents that are selective for their A blocks.[1−3] The copolymers in these systems self-assemble into independent spherical micelles which consist of a dense core of insoluble B blocks surrounded by a corona of flexible and highly swollen A blocks. A completely different behavior is expected in triblock copolymer systems mixed with a solvent that is selective for their midblocks. The polymer midblocks that emanate from the micellar core could form either loops or bridges, depending on whether the two end blocks of the copolymer are located in the same or in different domains. Little is known about the aggregation process and the subsequently formed microstructure in these systems. Interdomain bridging could be expected to result in the formation of clusters of interconnected domains possibly extending up to macroscopic length scales, thus providing the basis for physical gelation. Although such behavior had been ruled out in early experimental and theoretical studies,[4] it has recently been confirmed.[5−8]

These triblock copolymer gels have a unique behavior since the formation of the domain network is a thermoreversible process providing the basis for high elasticity. These systems combine characteristic properties of gels—like wetting and cohesive strength—with those of block copolymers—like formation of mesoscopic aggregates due to self-assembly. The elastic behavior of such systems has been recently described and attributed to the network structure without reference to the gel microstructure.[7] Very recently it has been demonstrated that under well-defined conditions the physical cross-links can even form highly ordered arrays.[9] This is quite surprising considering that individual microdomains are part of an extended network and displacement of a single domain should require the extraction of end-block chains located in neighboring domains.

In this paper we report the first in situ studies on the microstructure and mechanical properties of such physical gels. They were performed using time-resolved small-angle X-ray scattering (SAXS) experiments during extension at different rates on gel systems displaying either short- or long-range order. The long-range ordered lattice in such gels and its possible effect on the mechanical properties were also studied.

## 2. Experimental Part

**A. Gel Samples.** Polystyrene-poly(ethylene−butylene)-polystyrene triblock copolymers (SEBS) with a glassy/rubber like/glassy block sequence, dissolved in Fina oil A360, form systems in which a network of microdomains was detected by SAXS.[7] The gels are based on a SEBS with average molecular mass, styrene content, and polydispersity of 100 000, 29%, and 1.1, respectively.[10] The midblock selective solvent consists of a mixture of aliphatic and alicyclic compounds with average molecular mass around 400. Both components were mixed at 180 °C until a clear solution was obtained, which upon cooling to room temperature yielded transparent, highly elastic solids. Gels with copolymer contents of 7, 12, and 20 wt % (i.e., a total polystyrene content $\varphi_{PS}$ of 0.02, 0.0348, and 0.058, respectively) were investigated.

**B. Small-Angle X-ray Scattering.** SAXS experiments were performed on the X33 camera of the EMBL at HASYLAB on the storage ring DORIS III of Deutsches Elektronen Synchrotron (DESY), Hamburg, Germany.[11,12] The range of momentum transfer $q$ ($q = 4\pi \sin \theta/\lambda$, where $2\theta$ is the scattering angle and $\lambda$ the X-ray wavelength (0.15 nm)) covered was 0.03 nm$^{-1} \leq q \leq 3.0$ nm$^{-1}$. The structural development during continuous deformation was followed by recording scattering patterns in intervals of 10 or 20 s, depending on the deformation rate. The data were scaled to the primary beam intensity and corrected for detector response, and the background scattering was subtracted.

**C. Stress−Strain Experiments.** The home-built stretching device allowed stress−strain experiments at deformation rates, $r$, between $10^{-4}$ and $10^{1}$ s$^{-1}$. The sample was displaced with an accuracy of 1 $\mu$m via worm gear, driven by a computer-controlled stepping motor. To prevent movement of the central

* To whom correspondence should be addressed. Telephone: +32-16-327467. Fax: +32-16-327990. E-mail: Harry.Reynaers@chem.kuleuven.ac.be.
[†] Cathlolic University of Leuven.
[‡] Present address: FOM Institute for Atomic and Molecular Physics, Kruislaan 407, 1098 SJ Amsterdam, The Netherlands.
[§] DSM Research.
[∥] European Molecular Biology Laboratory, Hamburg Outstation.

S0024-9297(98)00116-8 CCC: $15.00 
Published on Web 08/06/1998

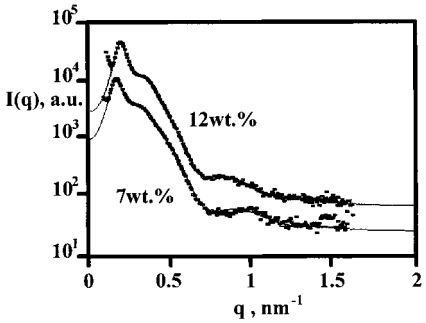


**Figure 1.** Scattering patterns obtained from SEBS-100 gels with 7 and 12 wt % copolymer at room temperature. Solid lines correspond to fits based on a Percus−Yevick hard-sphere model.[9]

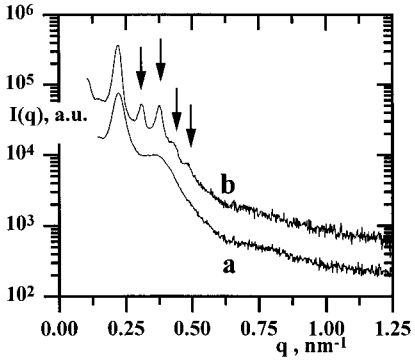


**Figure 2.** Scattering patterns of a SEBS-100 gel with 20 wt % copolymer (a) quenched from 140 °C and (b) quenched from 140 °C and subsequently annealed for 18 h at 90 °C. Measurements are done at room temperature. Arrows indicate the positions of the additional interference maxima in b.

part of the sample through which the X-ray beam passes, the stretching device is equipped with simultaneously moving sample clamps. Stresses during sample deformation are detected by a transducer with $10^{-2}$ N resolution. The position of zero elongation was adjusted to the strain value where stress sets in, and the position of the sample clamps was adjusted to obtain a steep stress increase near the zero position. During the deformation process, the sample was monitored using a video camera. Typical sample sizes used during those experiments were $20 \times 2 \times 15$ mm$^3$.

The small dimensions of the stress−strain device which was less than 10 cm along the beam path together with the strong scattering signal from the gel samples allowed us to perform stretching experiments at ambient conditions rather than under vacuum. This ruled out compositional changes due to solvent evaporation and resulted only in a minor increase of the background scattering.

## 3. General Part

**Morphology of Nondeformed Gel Systems: Influence of Thermal treatment on the Microstructure.** Scattering experiments were performed on nondeformed gels with polymer concentrations of 7, 12, and 20 wt % and solid to liquid transitions of around 80, 95, and 110 °C, respectively. A first set of measurements was made on samples that were heated to 140 °C and subsequently quenched to room temperature. The scattering patterns in Figures 1 and 2a are characterized by a form factor with a first side maximum around $q_{max} \sim 0.8$ nm$^{-1}$, corresponding to spherical polystyrene microdomains with core radii of $R_c = 5.76/q_{max} \sim 8$ nm and a structure factor with a maximum at $q^* \sim 0.2$ nm$^{-1}$ which have been explained elsewhere, using the hard-sphere liquid approximation.[8,13] In this model, the microstructure is represented by an assembly of short-range-ordered hard spheres with an effective radius $R_{hs}$ much larger than the actual radius of the polystyrene core, which accounts for the interactions between microdomains. A second parameter, $\phi_{hs}$, represents the volume fraction of the fictive hard spheres in the material. As illustrated in Figure 1, this model provides good fits to the scattering data with $\phi_{hs}$ values of around 0.3 at ambient temperatures. Compared to the volume fraction ($\phi_{hs} = 0.47$) where hard-sphere crystallization—and thus formation of long-range-ordered arrays of microdomains—takes place,[3] the values of $\phi_{hs}$ derived for the SEBS gel systems are low. A more pronounced structure factor[9] between 50 and 100 °C reflects an increased hard-sphere volume fraction in this temperature range. Consequently, the morphology of gel samples, especially with a copolymer content above 15 wt %, continues to evolve during annealing in this temperature range and displays the final morphology illustrated in Figure 2 for a gel with 20 wt % copolymer. During annealing at 90 °C reordering of the microdomains takes place, resulting in a long-range-ordered morphology. This is indicated by a slight decrease in width of the main structure factor maximum compared to the nonannealed system and the presence of additional interference maxima as illustrated in Figure 2. The positions of these interference maxima follows the sequence $1{:}\sqrt{2}{:}\sqrt{3}{:}\sqrt{4}{:}\sqrt{5}{:}\sqrt{6}$ characteristic of a cubic lattice. From the position of the first maximum at $q^* = 2\pi/a = 0.195$ nm$^{-1}$, one finds a lattice parameter $a = 32$ nm for a primitive lattice and $a = 2\sqrt{2}\pi/q^* = 45.5$ nm for a body centered cubic (bcc) lattice. The core radius $R_{core} = 5.76/q_{max}$, derived from the position of the first side maximum of the form factor at $q_{max} = 0.69$ nm$^{-1}$, is 8.3 nm. The microdomain volume fraction in the gel $\varphi$ was calculated for a primitive cubic lattice ($\varphi_{sc} = 4\pi/3(R_{core}/a)^3$ and for a bcc lattice ($\varphi_{bcc} = 8\pi/3(R_{core}/a)^3$). The volume fraction of polystyrene in a gel ($\varphi_{PS} = 0.058$) with 20 wt % copolymer, assuming complete microphase separation of the polystyrene end blocks, is closer to that calculated for a bcc morphology ($\varphi_{bcc} = 0.057$) than for a primitive lattice ($\varphi_{sc} = 0.072$). After quenching to room temperature, the body centered cubic morphology is stable for weeks, although the diffraction maxima slightly broaden directly upon cooling, probably due to stresses which build up in the network during quenching.

**Deformation of Gel Samples. (a) Stress−Strain Behavior.** The values for the extension at the breaking point of the gel samples are $\lambda_{break} = 1.8$ for nonannealed and around $\lambda_{break} = 2$ for annealed gels; values for their tensile strength are around $\sigma_{break} = 0.1$ MPa. This should be compared with values of $\lambda_{break} \sim 6$ and $\sigma_{break} \sim 10$ MPa typically for vulcanized rubber systems. Nevertheless, the stress−strain diagram recorded during uniaxial extension of the gels is nonlinear, which is a characteristic of the behavior of thermoplastic elastomers, and can be described by Mooney's relation[14]

$$\sigma(\lambda) = (2C_1 + 2C_2\lambda^{-1})(\lambda^2 - \lambda^{-1})$$

suggesting a plot of $\sigma(\lambda)$ ($\lambda 2 - \lambda^{-1}$) versus $\lambda^{-1}$, where $\sigma$ represents the true stress and $\lambda = L/L_0$ the extension ratio, as illustrated in Figure 3. The parameters $2C_1$ and $2C_2$ are constants, independent of the elongation ratio. At high deformations ($\lambda^{-1} \rightarrow 0$), the stress−strain data, represented in a Mooney plot, approach the

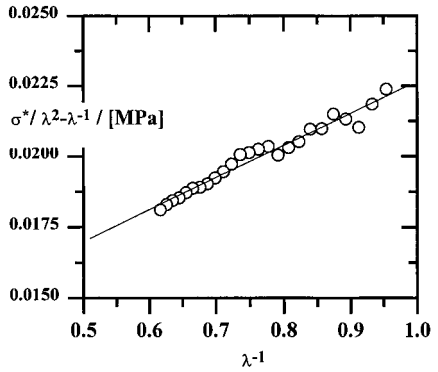


**Figure 3.** Mooney plot of the stress−strain data, recorded upon extension at an extension rate of $r = 4 \times 10^{-4}$ s$^{-1}$.

elasticity parameter $2C_1$ which is related to the molecular weight between cross-link points $M_c$

$$2C_1 = (1 - 2/f)\rho k_B T/M_c$$

where $\rho$ is the network density and $f$ represents the network functionality. In the present system the functionality is rather high and the $2/f$ term can be neglected. In the limit of small deformations ($\lambda^{-1} \rightarrow 1$), the curve approaches $2C_1 + 2C_2$. According to theories of rubber elasticity,[15] the ratio $2C_2/2C_1$ is a measure for the change from an affine to a nonaffine elastic deformation with increasing stress of the network where entanglement contributions become more pronounced. Long-range ordering of the microstructure in the preannealed gel sample does not significantly influence the stress−strain curve. The Mooney−Rivlin parameters $2C_1$ and $2C_2$, calculated from the stress−strain data, are 0.011 and 0.023 for the quenched system and 0.01 and 0.03 for the annealed one.

**(b) Evolution of the Microstructure under Deformation: Quenched Samples.** Figure 4 displays time-resolved scattering patterns, collected during deformation of the gels, which reveal a change of structural features on a length scale between 2.0 and 200 nm upon macroscopic deformation of the gel samples. The side maximum of the form factor maximum at $q_{max} = 0.69$ nm$^{-1}$ appears to be unchanged, indicating that the average size of the microdomains is not affected by deformation. The shift of the structure factor maximum toward lower $q$ values at higher extension reflects the increase in interdomain spacing along the deformation axis. Beyond the breaking point, it returns to its original position. The scattering experiments confirm that the self-assembled end-block domains represent the physical cross-links in a three-dimensional network and the midblock chains form the bridges between individual domains, thereby providing the basis for a highly interconnected three-dimensional network of microdomains.

The deformation of the microdomain network is affected by the macroscopic extension rate. The positions of the structure factor maxima $q^*$ are displayed as a function of the strain ratio $\lambda = L/L_0$ in Figure 5. The solid line indicates the limiting case of an affine behavior where the macroscopic deformation $\lambda$ results in a deformation of the microstructure by a value of $\lambda$ in the direction parallel (and $\sqrt{\lambda}$ perpendicular) to the deformation axis. At low deformation rates, the deformation of the microdomain network obviously deviates from the ideal behavior, as was also recently reported

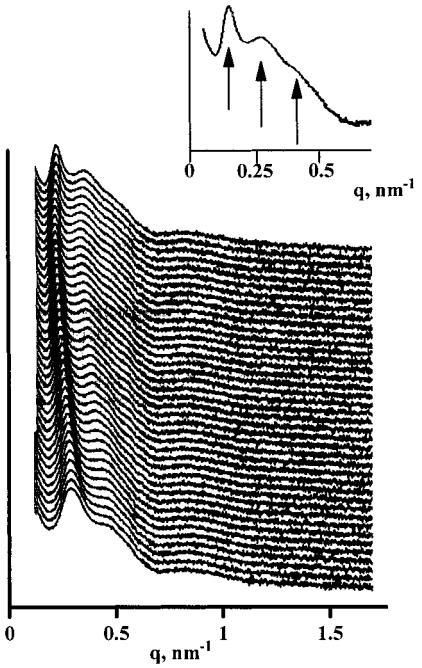


**Figure 4.** Time-resolved scattering patterns of a 20 wt % gel recorded during deformation from $\lambda = 1$ to 2 at an extension rate of $r = 4 \times 10^{-4}$ s$^{-1}$. The individual scattering profiles were recorded in 20-s intervals and are displaced along the ordinate for better visualization.

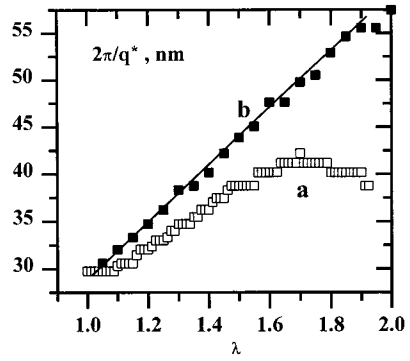


**Figure 5.** Spacings $d = 2\pi/q_{max}$, derived from the position of the structure factor maxima $q_{max}$ as a function of the deformation ratio $\lambda$. Extension rates were (a) $r = 4 \times 10^{-4}$ s$^{-1}$ and (b) $r = 10^{-2}$ s$^{-1}$.

for other gel systems.[7] In contrast, the results at the highest deformation rate in Figure 5 indicate that the deformation of the microstructure, judged from the positions of the structure factor maxima in the scattering patterns, is very close to that expected for an affine transformation.

At the highest deformation rates, another feature connected to the order in the physical network becomes obvious and additional, very weak structure factor maxima with spacing ratios corresponding to 1:2:3 (indicated by the arrows in the inset of Figure 4) appear in the scattering patterns. Such a behavior closely resembles scattering from a highly distorted layer-type structure[16] where the "layers" are oriented with their normal parallel to the deformation axis. Individual layers would be constituted by microdomains with a relatively large interdomain spacing in the direction parallel to the deformation axis, compared to the spacing perpendicular to it. The additional interference maxima should be due to ordering of the layers in the

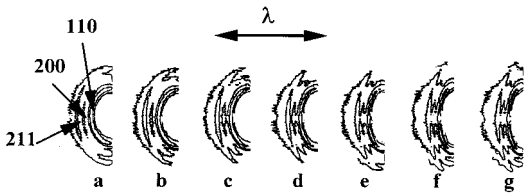


**Figure 6.** Contour plots of the two-dimensional scattering diagrams, recorded during deformation with $r = 4 \times 10^{-1}$ s$^{-1}$ at deformation ratios $\lambda = 1.1$ (a), 1.2 (b), 1.3 (c), 1.4 (d), 1.5 (e), 1.6 (f), and 1.7 (g).

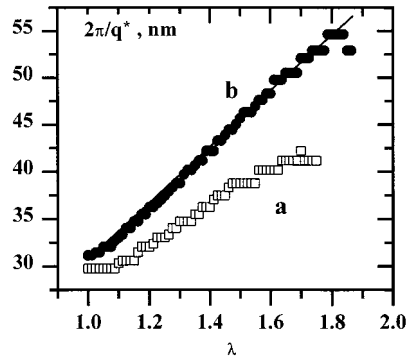


**Figure 7.** Spacings $q^*$, derived from the position of the structure factor maxima $q_{max}$ from a quenched sample (a) and a sample preannealed for 18 h at 90 °C (b). The extension rate was $r = 4 \times 10^{-4}$ s$^{-1}$.

stretching direction, which reaches a maximum just before the breaking point.

**(c) Evolution of the Microstructure under Deformation: Annealed Samples.** In a second step the effect of thermal treatment on the deformation behavior of the microstructure was investigated. The gel sample was preannealed for 18 h at 90 °C, and the body centered microstructure characterized by three interference maxima was obtained. Two-dimensional scattering patterns indicate the presence of a polycrystalline morphology where crystalline regions are randomly oriented with respect to each other. Such a polycrystalline morphology, rather than a single crystal-like structure, is not at all surprising since previous studies revealed that thermal treatment alone does not suffice to obtain single crystal-like structures.[9]

As the high solvent content in the present systems might promote a transformation of the polycrystalline microstructure at high deformation ratios, its possible influence was also investigated during deformation experiments. Figure 6 a−g displays the two-dimensional scattering pattern from a gel with bcc morphology recorded at various strain values, $\lambda$. Two features are apparent from the scattering pattern of the deformed gel. The first concerns the position of the interference rings: The shape of these rings clearly depends on the deformation ratio and transforms into an ellipsoid with its short axis oriented parallel to the deformation axis. As in the case of the nonannealed gel, this behavior indicates an increase of the distance between network junctions along the deformation axis, whereas the interdomain spacing decreases perpendicular to it. This indicates that in a gel with long-range-ordered cross-links the macroscopic deformations are transferred to the length scale of the interdomain spacing and result in a deformation of the unit cell. Figure 7 displays the dependence of the Bragg spacings on the strain ratios for annealed and nonannealed samples, both with a copolymer content of 20 wt % and subjected to the same deformation rate. Upon deformation, the annealed sample reveals an affine response of the microstructure that was observed only at higher extension rates with the nonannealed material.

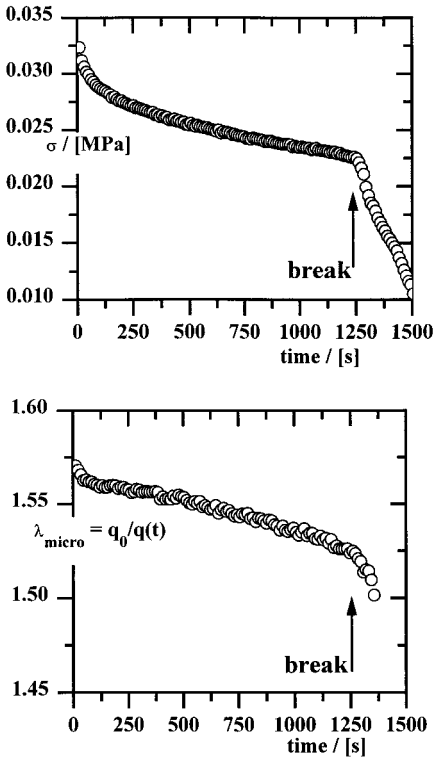


**Figure 8.** Time dependence of (a) the apparent stress $\sigma(t)$ and (b) the microscopic extension ratio $\lambda_{micro} = q_0/q(t)$, recorded after a step deformation at $\lambda = 1.66$.

The second feature is a significant change of the azimuthal intensity distribution of the interference maxima, indicating that macroscopic deformation results in a change of the electron density distribution within the body centered cubic network. Due to deformation the interdomain spacing decreases and the electron density perpendicular to the deformation axis becomes more uniform.

**(d) Relaxation in the Network Structure.** Another factor that could affect the type of deformation—affine or nonaffine—of the microstructure would be a structural relaxation which would take place in the sample upon deformation. In principle, this could be related to either a finite lifetime of the physical cross-links or a relaxation in the boundary regions between grains of the network that have a lower connectivity. As the experiments were performed under ambient conditions where the end blocks form glassy domains, the influence of a finite cross-link lifetime can be ruled out in favor of a relaxation in the regions of lower network connectivity. As shown in Figure 8, both stress and microstructure, recorded simultaneously on the same sample, reveal a relaxation process after a steplike deformation.

## 4. Conclusions

SEBS triblock copolymers dissolved in a solvent selective for their midblocks form microphase-separated polystyrene domains. At ambient temperatures, the glassy microdomains act as physical cross-links in a three-dimensional network, thereby providing the basis

for the formation of highly elastic gels. Since microstructural features are accessible by X-ray scattering, these gels are ideal model systems for in situ studies on the relations between stress−strain properties and microstructure, using time-resolved SAXS. Such simultaneous studies reveal that macroscopic sample deformations are transferred via the three-dimensional microdomain network to a microscopic level. Deformations at this microscopic level can be either nonaffine or affine, depending on the extension rate, whereas the short- or long-range ordering of the cross-links in the three-dimensional network depends on the thermal conditions. Deformation behavior of the gels with long-range cross-link order is nearly affine. For both affine and nonaffine transformations the stress−strain properties can be described, using the Mooney equation with only slightly different parameters.

**Acknowledgment.** The authors thank the European Union for support of the work at the EMBL through the HCMP Access to Large Installations Program (Contract No. CHGE-CT93-0040) and for Grant INTAS-96-1115. R.K. and N.M. are grateful to KULeuven for research fellowships. This work is part of a project supported by FWO-Vlaanderen.

## References and Notes

(1) McConnell, G. A.; Gast, A. P.; Huang, J. S.; Smith, S. D. *Phys. Rev. Lett.* **1993**, *71*, 2102−2105.
(2) McConnell, G. A.; Lin, M. Y.; Gast, A. P. *Macromolecules* **1995**, *28*, 6754−6764.
(3) Mortensen, K.; Pedersen, J. S. *Macromolecules* **1993**, *26*, 805−812.
(4) Tang, W. T.; Hadziioannou, G.; Cotts, P. M.; Smith, B. A.; Frank, C. W. *Polym. Prepr. (Am. Chem. Soc., Div.)* **1986**, *27* (2), 107−109.
(5) Balsara, N. P.; Tirrell, M.; Lodge, T. P. *Macromolecules* **1991**, *24*, 1975−1986.
(6) Nguyen-Misra, M.; Mattice, W. L. *Macromolecules* **1995**, *28*, 1444−1457.
(7) Quintana, J. R.; Diaz, E.; Katime, I. *Macromol. Chem. Phys.* **1996**, *197*, 3017−3026.
(8) Mischenko, N.; Reynders, K.; Mortensen, K.; Scherrenberg, R.; Fontaine, F.; Graulus, R.; Reynaers, H. *Macromolecules* **1994**, *27*, 2345−2347.
(9) Kleppinger, R.; Reynders, K.; Mischenko, N.; Koch, M. H. J.; Mortensen, K.; Reynaers, H. *Macromolecules* **1997**, *30*, 7008−7011.
(10) Patents EP-A-029978, U.S. 5,149,736 and WO-A-9305113; Shell Technical Bulletins SC 1102-89 and SC 198-92.
(11) Koch, M. H. J.; Bordas, J. *Nucl. Instrum. Methods* **1983**, *208*, 461−469.
(12) Boulin, C. J.; Kempf, R.; Gabriel, A.; Koch, M. H. J. *Nucl. Instrum. Methods* **1988**, *A269*, 312−320.
(13) Reynders, K.; Mischenko, N.; Kleppinger, R.; Mortensen, K.; Koch, M. H. J.; Reynaers, H. *J. Appl. Crystallogr.* **1997**, *30*, 684−689.
(14) Mooney, M. *J. Appl. Phys.* **1940**, *11*, 582−595.
(15) Flory, P. J. *Proc. R. Soc. London* **1976**, *A351*, 351−380.
(16) Mischenko, N.; Reynders, K.; Mortensen, K.; Overberg, N.; Reynaers, H. L. *J. Polym. Sci., Polym. Phys.* **1996**, *34*, 2739−2745.

MA9801164